

# New approach for the measurement of damping properties of materials using the Oberst beam

Jean-Luc Wojtowicki<sup>a)</sup>

*Henkel Surface Technologies, Automotive Division, Acoustic Center, 82 Avenue du 85 de Ligne, 58203 Cosne sur Loire, France*

Luc Jaouen<sup>b)</sup>

*Laboratoire d'Acoustique de l'Université du Maine, UMR CNRS 6613, 72085 Le Mans Cedex, France*

Raymond Panneton<sup>c)</sup>

*Groupe d'Acoustique de l'Université de Sherbrooke, Sherbrooke, Québec J1K 2R1, Canada*

(Received 28 October 2003; accepted 11 May 2004; published 26 July 2004)

The Oberst method is widely used for the measurement of the mechanical properties of viscoelastic or damping materials. The application of this method, as described in the ASTM E756 standard, gives good results as long as the experimental set-up does not interfere with the system under test. The main difficulty is to avoid adding damping and mass to the beam owing to the excitation and response measurement. In this paper, a method is proposed to skirt those problems. The classical cantilever Oberst beam is replaced by a double sized free-free beam excited in its center. The analysis is based on a frequency response function measured between the imposed velocity at the center (measured with an accelerometer) and an arbitrary point on the beam (measured with a laser vibrometer). The composite beam (base beam + material) properties are first extracted from the measurement by an optimization algorithm. Young's modulus and structural damping coefficient of the material under test can be deduced using classical formulations of the ASTM E756 standard for typical materials or using a finite element model for more complex cases. An application to a thick and soft viscoelastic material is presented, the results are shown to be consistent with Kramers-Kronig relations. © 2004 American Institute of Physics. [DOI: 10.1063/1.1777382]

## I. INTRODUCTION

The "Oberst beam" is a classical method for the characterization of damping materials based on a multilayer cantilever beam (base beam + one or two layers of other materials). As the base beam is made of a rigid and lightly damped material (steel, aluminum), the most critical aspect of this method is to properly excite the beam without adding weight or damping. So, exciting the beam with a shaker is not recommended because of the added mass (moving mass, stinger misalignment, force transducer). Alternative solutions are suggested in the ASTM E576 standard.<sup>1</sup> An electromagnetic noncontacting transducer (tachometer pick-up, for example) can provide good excitation but it is limited to ferromagnetic materials. As aluminum is widely used for the base beam, a small piece of magnetic material must be glued to achieve specimen excitation.

This method creates two other problems. The first one is the difficulty to properly measure the excitation force. If there is no contact, the injected force must be evaluated by the measurement of the voltage or current applied to the pick-up, without knowing what is really proportional to the applied force. Moreover, this system is linear for small am-

plitudes. As the measurement is made near resonances of the structure, it is not obvious that the hypothesis of linearity is respected. The second problem is the fact that the small piece of ferromagnetic glued to the structure is another source of uncertainty (added damping due to the gluing, mass of the added piece).

The measurement of the response of the beam is usually made using an accelerometer. Even if the problem of added damping and mass is much less critical because small and light accelerometers are available, it is preferable to avoid this solution for the same reasons as above. A straightforward solution is to use a laser vibrometer, which can accurately measure dynamic velocities with no contact. However, this equipment is much more expensive than a simple accelerometer.

Another problem can occur because of the clamped condition of the beam, see Fig. 1. The clamping is simulated by an increase of the thickness of the beam (the root). This root is wedged into a heavy and stiff clamping system. Usually this system is satisfactory but problems can occur in the case of misalignment, insufficient clamping force, and bad machining of the root.

The objective of this study is to develop an alternative to method the one proposed in the ASTM E756 standard,<sup>1</sup> in order to avoid experimental uncertainties and increase the precision of the measurement.

<sup>a)</sup>Electronic mail: jean-luc.wojtowicki@henkel.com

<sup>b)</sup>Electronic mail: luc.jaouen@univ-lemans.fr; Also at Groupe d'Acoustique, Université de Sherbrooke.

<sup>c)</sup>Electronic mail: raymond.panneton@usherbrooke.ca

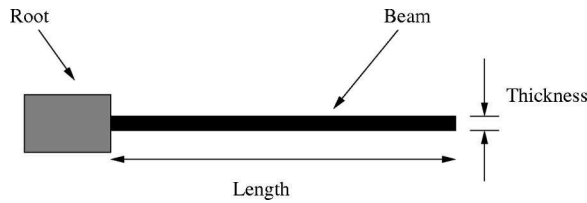


FIG. 1. Cantilever beam used in the Oberst method.

## II. PRINCIPLE

A cantilever beam has the same dynamical behavior than a free-free beam of twice the length excited in its center by a normal imposed displacement  $Y_0$ , see Fig. 2. In this case, only the even modes of the free-free beam will be excited, and its modal behavior will be similar to a clamped beam since the slope and the relative displacement to the imposed motion are null at this point.

An experimental set-up for the free-free beam excited in its center is proposed in Fig. 3. The beam under test (with or without damping material) is simply screwed in its center to an electrodynamic shaker by mean of a threaded rod. In practice this is easy to set up; however care must be taken on the precision of the location of the center to avoid an unbalanced system.

## III. THEORETICAL BACKGROUND

### A. Beam equation: Compact model

The bending vibrations of a beam are described by

$$Y(x, \omega) = C \cosh(\beta x) + D \sinh(\beta x) + F \cos(\beta x) + G \sin(\beta x) \quad (1)$$

with

$$\beta^4 = \frac{\rho A \omega^2}{EI}, \quad (2)$$

where  $C$ ,  $D$ ,  $F$ , and  $G$  are four unknown coefficients determined from boundary conditions,  $A$  is the cross-section area,  $\omega$  the pulsation,  $\rho$  the mass density of the beam,  $E$  the elastic modulus (or Young's modulus), and  $I$  the second moment of area of the beam cross section.

For the free-free beam problem shown in Fig. 2, the following four boundary conditions are used:

$$EI \frac{\partial^2 Y}{\partial x^2} = 0 \quad \text{at } x = 0 \text{ and } x = L, \quad (3)$$

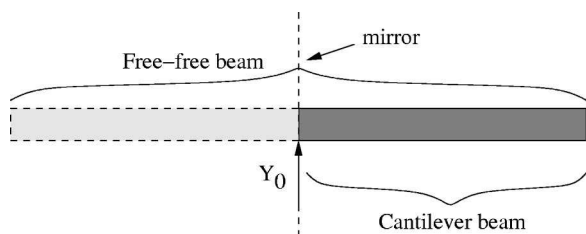


FIG. 2. Similarity between a free-free beam excited in its center and a cantilever beam excited by its base.

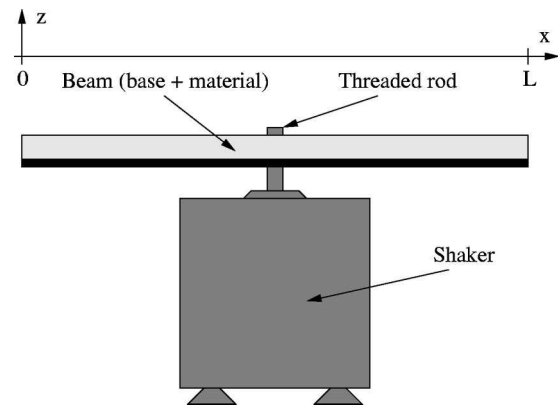


FIG. 3. Proposed experimental set-up: a composite beam excited in its center by a normal imposed displacement.

$$\frac{\partial}{\partial x} \left( EI \frac{\partial^2 Y}{\partial x^2} \right) = 0 \quad \text{at } x = 0 \text{ and } x = L, \quad (4)$$

where  $L$  is the length of the beam.

These equations represent the bending moment and the shear force at both extremities of the beam, respectively. Conditions at  $x=0$  lead to a simplification of Eq. (1):  $C=F$  and  $D=G$ .

The imposed displacement  $Y_0$  along the normal axis at the center point gives the following cinematic constraints to apply on Eq. (1):

$$Y(L/2) = Y_0, \quad (5)$$

$$\frac{\partial Y(L/2)}{\partial x} = 0. \quad (6)$$

Finally, if  $H$  is the ratio of the dynamic response of the beam divided by the imposed motion, Eqs. (1)–(6) yield to

$$H(x, \omega) = \frac{1}{2} \frac{\cosh(\beta L/2) + \cos(\beta L/2)}{1 + \cosh(\beta L/2)\cos(\beta L/2)} [\cosh(\beta x) + \cos(\beta x)] + \frac{1}{2} \frac{\sinh(\beta L/2) - \sin(\beta L/2)}{1 + \cosh(\beta L/2)\cos(\beta L/2)} [\sinh(\beta x) + \sin(\beta x)]. \quad (7)$$

In this equation, the natural frequency equation for a clamped-free beam of length  $L/2$  is found in the denominator. This confirms the validity of the principle of the method explained in Sec. II, in which the free-free beam excited in its center is similar to the Oberst beam.

It must be noted that the same model is used for both the bare beam and the composite beam. In the second case, the beam is seen as a homogenous equivalent beam. The objective is to determine the product  $E \times I$  of the beam under test where  $E$  is the complex equivalent Young's modulus:

$$E = E' (1 + j\eta) \quad (8)$$

with

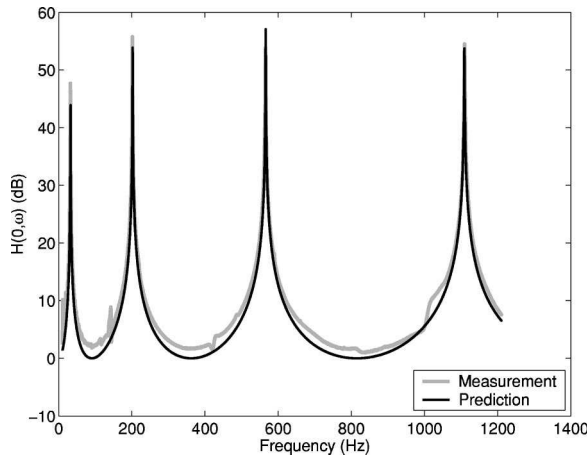


FIG. 4. Validation of the compact model, bare aluminum beam ( $L=400$  mm,  $w=19.97$  mm,  $H_1=1.58$  mm).

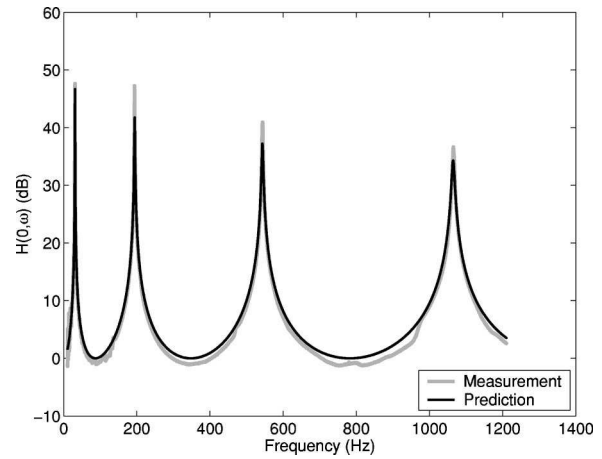


FIG. 5. Validation of the compact model, aluminum beam with an unknown adhesive layer ( $L=400$  mm,  $w=19.97$  mm,  $H_1=1.58$  mm,  $H_2=0.13$  mm).

- $E'$ : Real part of the Young's modulus,
- $\eta$ : Structural damping coefficient (real value).

$I$  is the equivalent second moment of area. The extraction of the material mechanical properties is made in a second step. Equation (7) is the "compact" model of the beam, because there is no need to make a modal decomposition, all the information is included in this single equation.

### B. Validation of the model

The model has been validated using two beams. The first one is a 400.00 mm long ( $L$ ) aluminum beam of 19.97 mm wide ( $w$ ) and 1.58 mm thick ( $H_1$ ). The real part of its Young's modulus  $E_1$  is 70.0 GPa and its structural damping coefficient  $\eta_1$  is 0.0007. These values have been taken constant for preliminary validation purposes. The results are given in Fig. 4 for a measurement point at the tip  $x=0$  of the beam. The agreement between the model's prediction and the measurement is good. The modal peaks are well located, the measured and calculated levels are close. The measured curve is obtained using the set-up depicted in Fig. 3. Experimental set-up will be discussed in detail in Sec. IV.

The frequency response function (FRF) between the middle point where the beam is excited and the tip of the beam tends towards 1 (0 dB) between two modes, the two points are vibrating in phase with the same amplitude. Near a mode, the response point reaches high amplitudes controlled by the damping. The frequencies of the modes could be predicted using the classical formulation for a cantilever beam. Conversely, those FRFs can be used directly to calculate the mechanical properties of materials using the ASTM E756 standard for example.

The second example (Fig. 5) is the result of the measurement on the same beam with an unknown double sided adhesive of thickness  $H_2=0.13$  mm. The Young's modulus has been adjusted, for the first mode, to obtain an equivalent complex modulus  $E$  allowing a good fitting of the calculated curve with the measured one for the first resonance. The fact that the real part of the Young's modulus and the damping coefficient of the composite beam are not constant cannot be clearly seen on this scale although it can be verified. This

example shows that the compact model can also be used for composite beams. In the following, the results will not be presented on such a wide frequency band. They will concentrate on each mode separately, in order to obtain at least one value for the damping and Young's modulus for each mode.

The advantage of this method is to calculate the properties of the composite beam using several data points and the real analytical formulation for the curve fitting. The ASTM E756 standard uses the values of the modal frequencies (read at the peaks) and damping (measured with an  $n$  dB bandwidth method). The modal frequency is equal to the peak frequency as long as the damping is light, in the case of high damping, the natural frequency should be corrected. Secondly, the  $n$  dB bandwidth method is a quick way to evaluate the damping and, actually, is not very precise. A curve fitting method is preferable. However, usual curve-fitting algorithms are based on trial functions, which are not the real function. The second objective of this work is to improve the precision of the determination of materials properties using a function which depicts the real physical problem: Eq. (7).

### C. Calculation of material properties

In the following, the approach is the same as the ASTM E756 standard, the calculation of material properties are based on the same models. The only difference is that the ASTM E756 standard separates the Young's modulus (real number) to the damping (real number) and makes two calculations. In this study, all the moduli are complex numbers.

#### 1. Extensional damping

When the damping material is unconstrained (glued on one or two faces of the base beam), the treatment is called extensional damping. As one of the faces of the material is free, the added rigidity is due to the bending. The determination of the materials properties is based on the Ross, Ungar, and Kerwin<sup>2,3</sup> model for a multilayer structure. The referred model allows to calculate the flexural rigidity  $E \times I$  of a multilayer beam or plate using the properties of the different layers (density, thickness, length, Young's or shear modu-

lus). The following equations give the equivalent flexural rigidity for a single sided damped beam and a double sided damped beam, respectively:

$$EI = E_1 I_1 \left( 1 + eh^3 + 3(1+h)^2 \frac{eh}{1+eh} \right), \quad (9)$$

$$EI = 2E_2 I_2 + E_1 I_1, \quad (10)$$

with  $e$ , Young's modulus ratio  $E_2/E_1$ ;  $h$ , thickness ratio  $H_2/H_1$ ;  $E_1$ , Young's modulus of the base beam ( $\text{N.m}^{-2}$ );  $I_1$ , second moment of area of the base beam cross section ( $\text{m}^4$ );  $H_1$ , thickness of the base beam (m);  $E_2$ , Young's modulus of the tested material ( $\text{N.m}^{-2}$ );  $I_2$ , second moment of area of the tested material cross section ( $\text{m}^4$ );  $H_2$ , thickness of the tested material (m).

The calculation of the Young's modulus of the material  $E_2$  using Eq. (9) leads to the resolution of an equation of the second order (two complex roots). But only the root with the positive real and imaginary part is the physical solution.

## 2. Shear damping

When the material is constrained between the base beam and a rigid layer, the composite beam has a slightly higher flexural rigidity due to the shear deformation of the sandwiched material, which is much higher than the bending deformation alone. Equation (11) (Ref. 3) gives the flexural rigidity for a composite beam with a shear damping treatment assuming that the base beam and the rigid constraining layer are similar,

$$EI = \frac{E_1 I_1}{6} + E_1 H_1 (H_1 + H_2)^2 \frac{G_2}{E_1 H_1 H_2 \beta^2 + 2G_2} \quad (11)$$

with  $G_2$  the complex shear modulus of the tested material ( $\text{N.m}^{-2}$ ).

The second term of Eq. (11) is due to the flexural rigidity of the sandwiched material. For soft material, this term can be neglected for the first modes. However, it is interesting to note that the shear deformation energy decreases as the frequency increases due to the division by the squared modal constant.

The complex Young modulus (or shear modulus) can be extracted from Eqs. (9) to (11) when the composite flexural rigidity  $E \times I$  has been previously determined by the curve fitting of Eq. (7) with experimental measurements for each frequency band containing one vibration mode. It must be noted that expressions (9)–(11) depend on assumptions detailed in Refs. 1 and 3.

## IV. APPLICATION

Estimations of the Young's modulus and the structural damping coefficient of a polyvinyl chloride based viscoelastic material are presented as an application of the proposed experimental set-up. This material of density  $1260 \text{ kg.m}^{-3}$  will be named material  $R$  in the following.

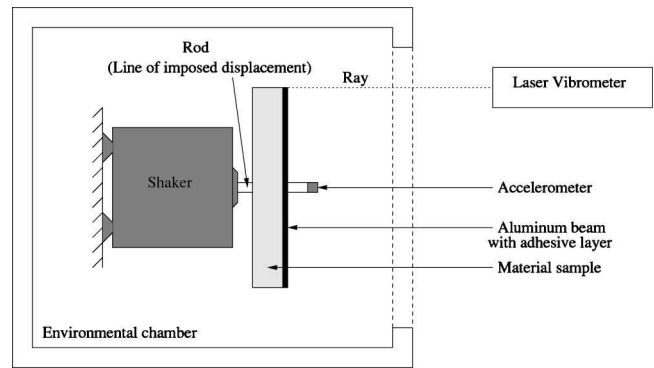


FIG. 6. Experimental set-up.

## A. Preparation of experiments

### 1. Selection of test configuration

The first step is to select the most appropriate beam configuration for the test. If the material under test is rigid enough to be measured alone, this is the best way to proceed. If not, it is suggested to start with the sandwich composite beam for softer materials like thin elastic materials. For heavier or more rigid materials (damping sheets), the single side beam can be tried, but the base beam should be as thin as possible and should never be thicker than the material under test. Globally, the ASTM E756 recommendations must be followed.

From static observations, the one side configuration is chosen for material  $R$ .

### 2. Gluing

The gluing of the material under test is another source of error. Some materials are self-adhesive, and in some cases the glue is not strong enough to insure a good contact between the two surfaces. In the case of slipping, the imposed deformation from the base beam to the material can lead to a slight underestimation of the properties of the material. Thin double sided adhesives can be used but great care must be taken as the adhesive layer's presence can affect the results. Particularly, it must be kept to a minimum thickness as recommended in the ASTM E756 standard.

To insure that the gluing of material  $R$  is sufficient, the double sided adhesive presented in Sec. III B is used. Preliminary tests have shown that the adhesive layer modify the response of the beam (see Fig. 5 compared to Fig. 4). A first inversion, using the method described in Sec. III C 1, is thus realized to estimate an equivalent Young's modulus and structural damping coefficient for the aluminum beam with adhesive layer.

## B. Experimental set-up

The experimental set-up is shown in Fig. 6. The damping layer is glued to the aluminum beam with a thin double sided adhesive. An electrodynamic shaker driven by a white noise signal excites the multilayer in its center through a line displacement. The tip motion is measured with a laser vibrometer and the center motion using an accelerometer. To obtain displacements, one time integration and a double time inte-

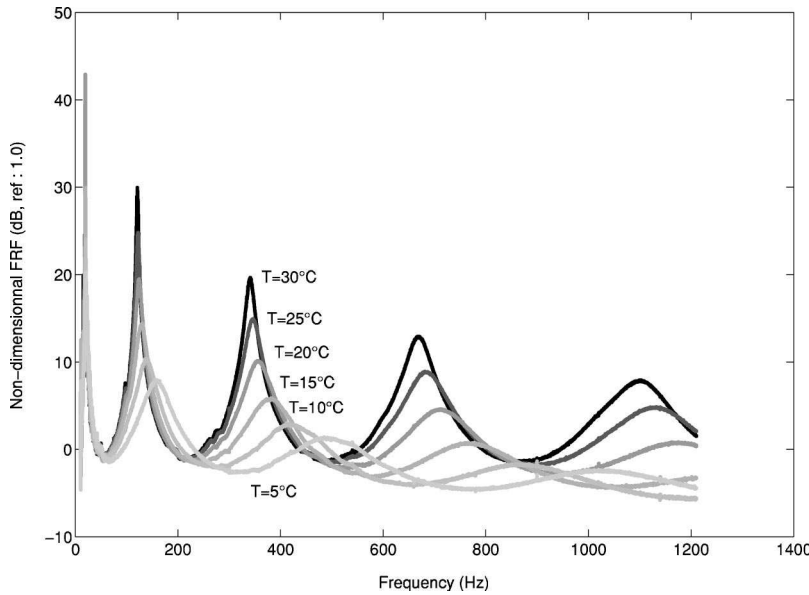


FIG. 7. Measured frequency responses for a one side configuration beam with viscoelastic material  $R$  as a function of frequency and temperature.

gration are performed on the laser vibrometer signal, and on the accelerometer signal, respectively.

Note that the rod's diameter must be minimum to support the accelerometer and impose the local displacement.

Measurements have been realized between 980–1000 mbar of static pressure with 10%–20% of relative humidity.

### C. Results

Figure 7 presents six FRF measurements obtained for material  $R$  at temperatures from 30°C to 5°C. In this figure, the frequency and temperature dependence of the material's stiffness and its structural damping is clear. The viscoelastic material stiffness decreases with temperature.

The thickness of the material sample is 6.35 mm (1/4 in.). The classical analysis for thin beams described in Sec. III C or in the ASTM E756 (Ref. 1) standard is not relevant for such a thickness. Consequently, a hierar-

chical three-dimensional finite element software<sup>4</sup> is used in the inversion to model the material  $R$  perfectly bonded onto the equivalent beam defined in Sec. III B. A quasistatic measure<sup>5</sup> of material  $R$  Poisson ratio  $\nu_{xz}$  reveals an elastic anisotropy, 0.11. Although this value is not usual, it will be used in the 3D simulation and assumed to be real and constant in the frequency range of interest and in temperature. This latter assumption can be challengeable.<sup>6</sup>

The rigidity of the previous base beam, with a double sided adhesive layer, is compared to the added rigidity due to the material  $R$  under test. These comparisons at various frequencies and temperatures allow to characterize material  $R$  elastic properties.

Figure 8 shows the variation of the real part of the Young's modulus, in the  $x$ -direction, with frequency and temperature for material  $R$ :  $E'_3$ . These results are obtained from measurements of Fig. 7 and the use of a Levenberg–Maquardt inversion algorithm.<sup>7,8</sup> The figure confirms the ear-

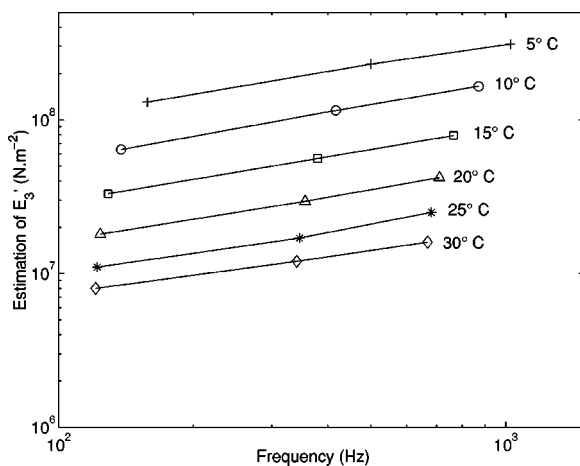


FIG. 8. Variations of the real part of Young's modulus  $E'_3$  with frequency and temperature for viscoelastic material  $R$ . +: 5°C, ○: 10°C, □: 15°C, △: 20°C, ★: 25°C, ◇: 30°C. Measurement points for each temperature are linked for the sake of legibility, not to suggest a linear evolution between these points.

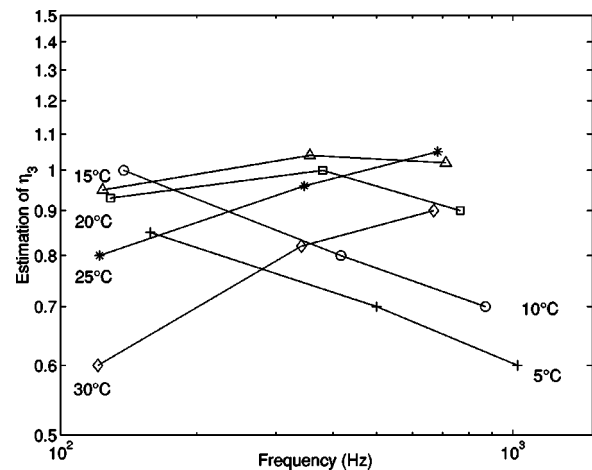


FIG. 9. Variations of the structural damping coefficient  $\eta_3$  with frequency and temperature for viscoelastic material  $R$ . +: 5°C, ○: 10°C, □: 15°C, △: 20°C, ★: 25°C, ◇: 30°C. Measurement points for each temperature are linked for the sake of legibility, not to suggest a linear evolution between these points.

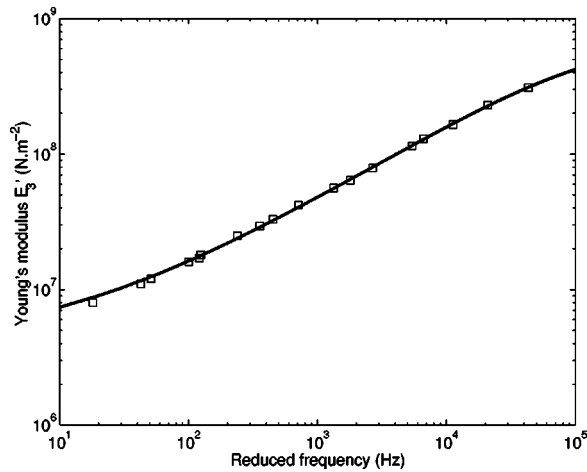


FIG. 10. TTS application: master curve of the real part of Young's modulus ( $E'_3$ ) real part at a reference temperature of 20°C for material  $R$ .  $\square$ : measurements, —: curve fitting of the fractional Zener model (Ref. 13).

lier observations: the material's modulus decreases significantly with temperature.

The variation of structural damping  $\eta_3$  with frequency and temperature, for this viscoelastic material, is shown in Fig. 9. One should note that the damping coefficient values for material  $R$  are high. Such damping values have, however, been previously reported (see Refs. 9 and 10 for example). A material's state transition, which will be more clearly highlighted in Fig. 11 of Sec. IV D, can also be observed.

In these two series of results, Figs. 8 and 9, the first mode results have been ignored because of high sensibility of this mode to boundary conditions. The same coefficients of variation as in the ASTM E756 standard applied on the precisions of these results, i.e., 10%–20%.

#### D. Validation

The consistency of measurement data for material  $R$  are discussed looking in Figs. 10 and 11. These figures show results of the time–temperature superposition (TTS) principle application for material  $R$ .<sup>11,12</sup>

A curve fitting for the real part of the Young's modulus,  $E'_3$ , using the fractional Zener model<sup>13</sup> with parameters  $M_0 = 3.98 \times 10^6 \text{ N.m}^{-2}$ ,  $c=202$ ,  $\alpha=0.553$ , and  $\tau=1.82 \times 10^{-6} \text{ s}$  is done in Fig. 10.

In Fig. 11, measurements of the structural damping coefficient  $\eta_3$  are compared with the theoretical calculation using the local Kramers–Kronig relations from dispersion of

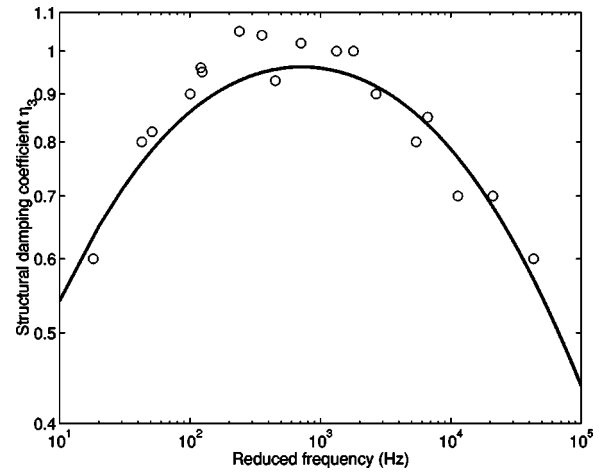


FIG. 11. TTS application: master curve of the structural damping coefficient  $\eta_3$  at a reference temperature of 20°C for material  $R$ .  $\circ$ : measurements, —: calculation using the local Kramers–Kronig relations from dispersion of the Young's modulus.

the Young's modulus.<sup>13</sup> The value of  $\alpha$  greater than 0.5 and the low accuracy of structural damping coefficient measurements can explain the underestimation of the theoretical calculus.<sup>13</sup>

#### ACKNOWLEDGMENT

The authors would like to thank Christian Langlois for his precious help on the numerical calculus.

- <sup>1</sup>ASTM E756-98, *Standard test method for measuring vibration-damping properties of materials* (American Society for Testing and Materials, 1998).
- <sup>2</sup>R. Ross, E. E. Ungar, and E. M. Kerwin, *Damping of plate flexural vibrations by means of viscoelastic laminate, Structural Damping, Proceedings of ASME* (New York, 1959).
- <sup>3</sup>A. D. Nashif, D. I. G. Jones, and J. P. Henderson, *Vibration Damping* (Wiley, New York, 1985).
- <sup>4</sup>C. Langlois, "Modelling vibro-acoustic problems with finite elements", Master's thesis University of Sherbrooke - Qc, Canada, 2003.
- <sup>5</sup>C. Langlois, R. Panneton, and N. Atalla, *J. Acoust. Soc. Am.* **110**, 3032 (2001).
- <sup>6</sup>T. Pritz, *Appl. Acoust.* **60**, 279 (2000).
- <sup>7</sup>K. Levenberg, *Q. Appl. Math.* **2**, 164 (1944).
- <sup>8</sup>D. W. Marquardt, *SIAM (Soc. Ind. Appl. Math.) J. Appl. Math.* **11**, 431 (1963).
- <sup>9</sup>D. I. G. Jones, *J. Sound Vib.* **140**, 85 (1990).
- <sup>10</sup>T. Pritz, *J. Sound Vib.* **246**, 265 (2001).
- <sup>11</sup>J. D. Ferry, *Viscoelastic Properties of Polymers* (Wiley, New York, 1961).
- <sup>12</sup>R. D. Corsaro and L. H. Sperling, *Sound and Vibration Damping with Polymers* (American Chemical Society, Washington, D.C., 1990).
- <sup>13</sup>T. Pritz, *J. Sound Vib.* **228**, 1145 (1999).